doi:10.1016/j.jmb.2005.08.037 J. Mol. Biol. (2005) 353, 104–115

JMB

Available online at www.sciencedirect.com

SCIENCE DIRECT®

ELSEVIER

Crystal Structures of a High-affinity Macrocyclic Peptide Mimetic in Complex with the Grb2 SH2 Domain

Jason Phan[1], Zhen-Dan Shi[2], Terrence R. Burke Jr[2] and David S. Waugh[1]*

[1]*Macromolecular Crystallography Laboratory Center for Cancer Research National Cancer Institute at Frederick, P.O. Box B, Frederick MD 21702-1201, USA*

[2]*Laboratory of Medicinal Chemistry, Center for Cancer Research, National Cancer Institute at Frederick, P.O. Box B, Frederick, MD 21702-1201 USA*

**Corresponding author*

The high-affinity binding of the growth factor receptor-bound protein 2 (Grb2) SH2 domain to tyrosine-phosphorylated cytosolic domains of receptor tyrosine kinases (RTKs) is an attractive target for therapeutic intervention in many types of cancer. We report here two crystal forms of a complex between the Grb2 SH2 domain and a potent non-phosphorus-containing macrocyclic peptide mimetic that exhibits significant anti-proliferative effects against erbB-2-dependent breast cancers. This agent represents a "second generation" inhibitor with greatly improved binding affinity and bio-availability compared to its open-chain counterpart. The structures were determined at 2.0 Å and 1.8 Å with one and two domain-swapped dimers per asymmetric unit, respectively. The mode of binding and specific interactions between the protein and the inhibitor provide insight into the high potency of this class of macrocylic compounds and may aid in further optimization as part of the iterative rational drug design process.

Published by Elsevier Ltd.

Keywords: Grb2 SH2; domain-swapped; macrocyclic tetrapeptide mimetic; S1s; drug design

Introduction

The down-regulation of protein-tyrosine kinase (PTK)-dependent signaling is a promising approach for the treatment of a variety of proliferative diseases, which is beginning to be fulfilled by PTK kinase inhibitors such as Gleevec[1] and CEP-701 (phase II trial).[2] An alternative and potentially complementary way of down-regulating PTK-dependent signaling is to interfere with protein–protein interactions downstream of the PTKs that are mediated by phosphotyrosyl (pTyr)-binding modules such as SH2 domains and phoshotyrosyl-binding (PTB) domains.[3] The growth factor receptor-bound protein 2 (Grb2) SH2 domain is an appealing example of this type of target because of its central role in signal transduction associated with several cancers, including breast cancer[4] and kidney cancers that are dependent on hepatocyte growth factor (HGF) signaling through the Met PTK (c-Met).[5] A significant effort has been devoted to the development of SH2 domain-signaling antagonists,[6,7] including the Grb2 SH2 domain.[8] The discovery of small molecules that bind to the Grb2 SH2 domain has been aided by the availability of NMR[9,10]and X-ray crystal structures[11–15] of high-affinity ligands bound to the protein. Here, we describe the structural basis for the binding of a macrocyclic peptide mimetic that exhibits low nanomolar Grb2 SH2 domain binding affinity. This inhibitor is remarkable not only for its binding potency, but also for its ability to block the association of Grb2 with activated cytoplasmic growth factor receptor PTK when administered to whole cells at sub-micromolar concentrations without the aid of prodrug derivatization or the use of artificial carrier techniques.[16]

Unlike most SH2 domains, which bind pTyr-containing peptides in extended conformations, ligands bind to Grb2 SH2 domains in type I β-turns with the pTyr and specificity-determining Asn residues being located at the i and $i+2$ positions, respectively.[11] This unique mode of

Abbreviations used: RTK, receptor tyrosine kinase; Grb2, growth-factor receptor-bound protein 2; NMA, normal mode analysis; pY and pTyr, phosphotyrosine; PTB, phophotyrosine-binding; PTK, protein-tyrosine kinase; Pmf, *p*-malonylphenylalanine; Pmp, 4-(phosphonomethyl)phenylalanine; r.m.s.d., root-mean-square deviation; SH2, Src homology 2; ORF, open reading frame.

E-mail address of the corresponding author: waughd@ncifcrf.gov

0022-2836/$ - see front matter Published by Elsevier Ltd.

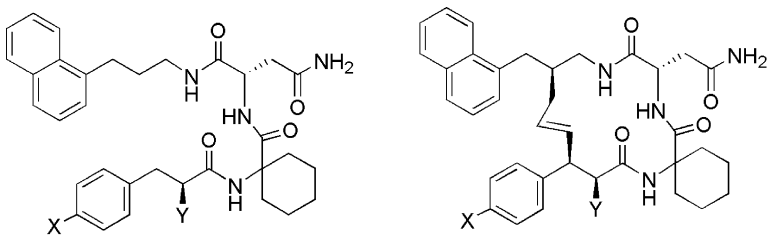

1 X = -O-P(O)(OH)$_2$; Y = -NHAc
2 X = -CH$_2$-P(O)(OH)$_2$; Y = -CH$_2$CO$_2$H
3 X = -CH$_2$-P(O)(OH)$_2$; Y = -CH$_2$CO$_2$H
S1s X = -CH(CO$_2$H)$_2$; Y = -CH$_2$CO$_2$H

Figure 1. Structures of the Grb2 SH2 domain-binding inhibitors discussed in the text.

binding is stabilized by van der Waals contacts with Trp EF1 (W121) (notation as proposed [17–19]). Starting from a minimal Grb2 SH2 domain-binding peptide, Ac-pTyr-Ile-Asn-Val-NH$_2$, Novartis Corp. made a series of systematic modifications to improve the binding affinity.[8] This led to the replacement of the pTyr+1 Ile with a 1-amino cyclohexane carboxylic acid residue (Ac$_6$c) that enhanced affinity by promoting a β-turn through a local 3_{10} helical conformation and by increasing hydrophobic contacts with protein residues.[20] In order to improve interactions with a hydrophobic region on the surface of the protein, the Val residue was replaced with a 3-naphthalen-1-yl-propyl group.[21] These modifications were combined to yield the peptide mimetic 1 (Figure 1), which exhibited significantly enhanced binding affinity relative to the starting minimal tetrapeptide.

Through a series of systematic modifications, Burke and co-workers transformed structure 1 first to the open-chain structure 2, and then to the macrocycle structure 3.[22] More recently, structure 3 was modified by replacement of its pTyr mimetic phosphonate group with a 2-malonyl moiety to yield macrocycle S1s.[16] This modification was predicated on the high Grb2 SH2 domain-binding affinity obtained when the phosphonomethyl-phenylalanyl (Pmp) residue of peptide 2 was replaced with *p*-malonylphenylalanine (Pmf).[23] S1s is remarkable for its high Grb2 SH2 domain-binding affinity in extracellular assays and its potency in whole cells. Structurally, it is noteworthy for combining three important features into a single molecule: (1) a malonyl-based phosphoryl mimetic; (2) an α-CH$_2$CO$_2$H moiety in the pTyr-mimicking portion; and (3) a macrocyclic structure derived from RCM-ring closure of a β-substitued pTyr mimetic. In light of its unusual structure, it was of interest to determine the manner of its binding. Accordingly, here we report the crystal structure of S1s in complex with the Grb2 SH2 domain.

Results

General description of the structures

Grb2 SH2 domain structures derived from two crystal forms ($C222_1$ and $F222$) were found to be consistent with the known fold; namely, a three-stranded antiparallel β-sheet sandwiched between an N-terminal α-helix (αA) and a C-terminal α-helix (αB). However, in both structures the αB helix is donated by a neighboring molecule, resulting in a domain-swapped dimer. This mode of dimerization has been observed before in a structure of the unligated Grb2 SH2 domain (PDB code 1JYU)[15] and in a complex between the Grb2 SH2 domain and a c-Met-derived tetrapeptide (PDB code 1FYR).[14] In all cases, the C-terminal helix becomes detached from the rest of the molecule and stretched toward the other subunit, placing the EF, βF, and FB loops in an extended conformation starting from the hinge point at Trp EF1 (W121) (Figure 2).

The superposition of the α-carbon traces of the four chains from the $C222_1$ structure, two from the $F222$ structure, four from the 1FYR structure, and one from the 1JYU structure is shown in Figure 2(d). These differ primarily in the BC loop of the core domain and the entire swapped domain after residue Trp EF1 (W121). The core domain amino acid residues 60–120 of the space group $C222_1$ subunit A were used as a reference. The α-carbon trace of the $C222_1$ subunit C and the $F222$ subunit A were aligned with r.m.s.d. values of 0.23 Å and 0.22 Å, while the values for the $C222_1$ subunits B and D, and the $F222$ subunit B were 1.21 Å, 1.05 Å, and 0.56 Å, respectively. The four chains from 1FYR and one chain from 1JYU were aligned with r.m.s.d. values in the 0.54 Å–0.65 Å range. The BC loop is in an open conformation in the $C222_1$ subunits B and D, and disordered in the $F222$ subunit B, while the subunits A and C in both space groups along with all four chains in 1FYR assume a closed conformation, which allows for interactions with the ligand (see below). The BC loop in the apo structure 1JYU adopts an intermediate position, with its Ser BC2 (S90) side-chain, depicted as a ball-and-stick model, pointing away from the ligand. The Trp EF1 (W121) side-chains in the $C222_1$ subunits A and C, the $F222$ subunit A, the 1FYR subunit D, and the apo 1JYU adopt an open orientation, while other chains rotate 120° to allow contact with the α and β methylene groups of the pY+2 Asn, thereby stabilizing the β-turn conformation.

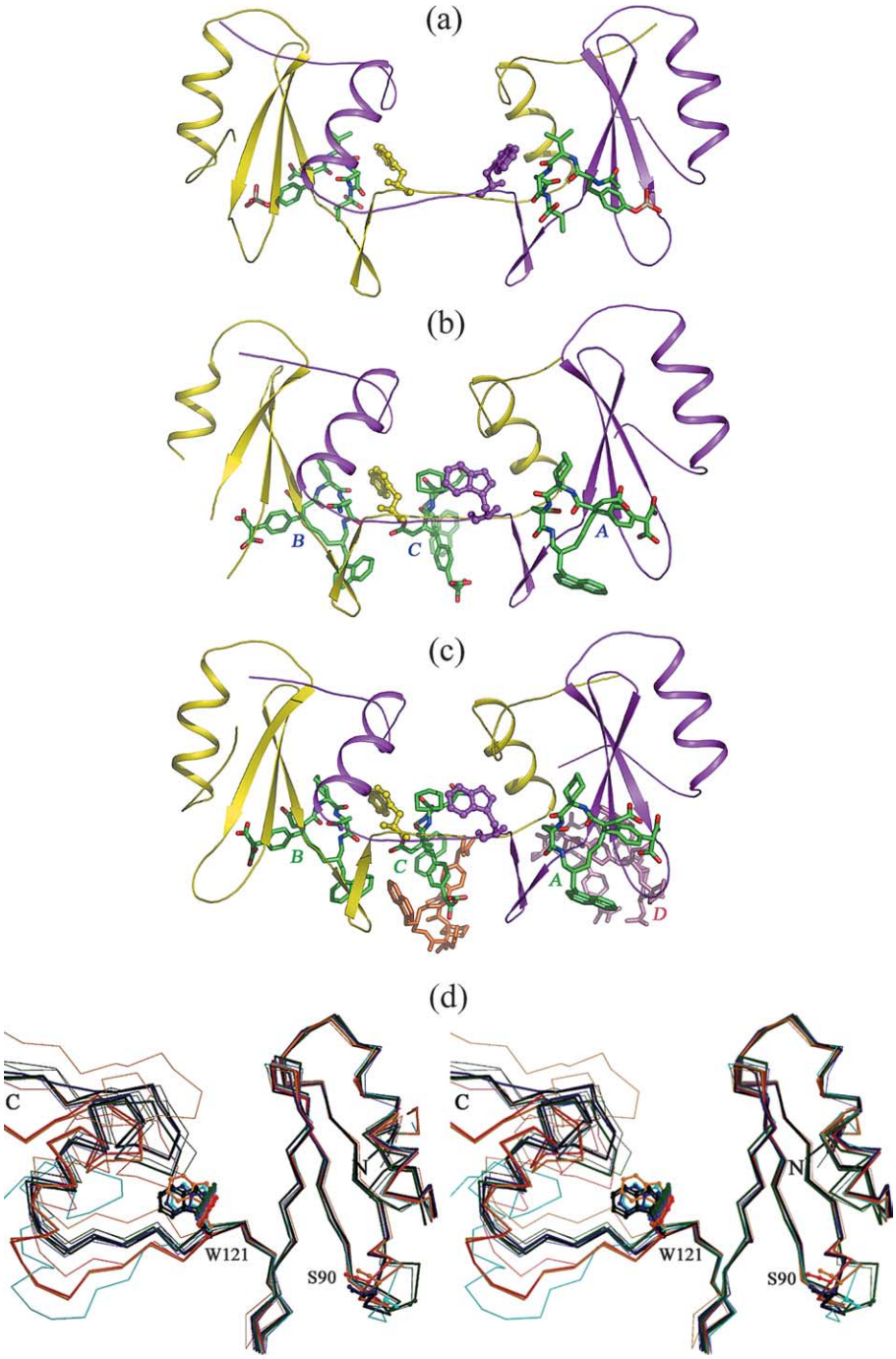

Figure 2. Ribbon representations of the domain-swapped dimer of Grb2 SH2 in complex (a) with the c-Met-derived peptide (PDB code 1FYR), (b) with the macrocyclic tetrapeptide mimetic S1s in space group *F*222, and (c) $C222_1$. The two domains are colored yellow and magenta and the ligands are depicted in ball-and-stick format. The β-turn stabilizing Trp EF1 (W121) is also displayed in ball-and-stick format. (d) Stereo view of the superposition of the α-carbon trace of $C222_1$ subunits A, B, C, D in black, dark green, thin black, thin dark green; *F*222 subunits A, B in dark blue, think blue; 1FYR subunits A, B, C, D in red, dark orange, thin red, thin orange; 1JYU chain A in cyan, respectively.

Ligand binding interactions in the pTyr-binding site

The potent macrocylic Grb2 SH2 antagonist S1s binds to the pTyr target site in a mode very similar to that of the tetraphosphopeptide Ac-pTyr-Ile -Asn-Val. The hydrogen-bonding schemes for the inhibitor in $C222_1$ subunits A and B are shown in Figure 3(a) and (b), respectively. The N-terminal –CH_2CO_2H group makes a salt-bridge to the guanidino group of Arg A2 (R67) in a fashion reminiscent of the *N*-acetyl carboxyl in 1FYR. The NH1 atom of Arg A2 (R67) also forms a hydrogen bond with an O atom derived from the

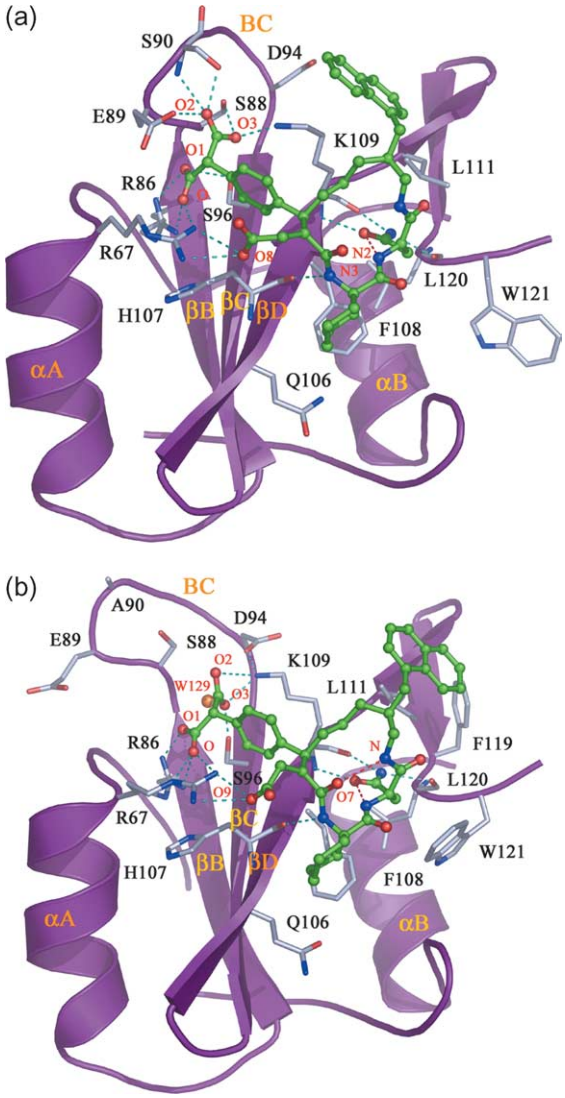

Figure 3. Diagrams of the hydrogen bonding networks in the active site of (a) subunit A and (b) subunit B with the Grb2 SH2 domain represented in cartoon, ligand-binding residues in bonds with grey carbon atoms, and ligands in ball-and-stick with green carbon atoms. Hydrogen bonds are in cyan broken lines and intramolecular bonds in red. Selected atoms of S1s are labeled in red.

malonyl-based phosphoryl mimetic but, unlike 1FYR, its NH rotates away from the ligand (Figure 3(a)). Arg B5 (R86) forms a bidentate salt-bridge with the malonyl O and O1 atoms, which is also hydrogen-bonded to the OG atom of Ser C3 (S96). The malonyl O and O1 atoms are superimposable on the phosphoryl O2P and O1P atoms of pTyr residues in other complexes. As for the other malonyl carboxylate group, the O2 hydrogen bonds with OE2 of Glu BC1 (E89), and the amide NH and OG of Ser BC2 (S90), while O3 interacts with OG of Ser B7 (S88) and NZ of Lys D6 (K109). Of note, the Glu BC1 (E89) and Lys D6 (K109) side-chains do not interact with the corresponding oxygen atoms in complex structures containing phosphate-based inhibitors. In these structures, the OG of Ser B7 (S88) hydrogen bonds to the phosphoryl ester oxygen. Therefore, there is a net gain of one ionic bond by the malonyl moiety as compared to the phosphoryl species and this originates from the Pmf O3 and Lys D6 (K109) NZ atoms. The equivalent residue, Lys60, in the Lck SH2 domain interacts with the 3′-phosphono group of 3′,4′-diphosphonophenylalanine,[24,25] and Lys62 in the pp60$^{c\text{-}Src}$ SH2 domain when binding citrate and malonate ions.[26] In the current structure, this interaction helps to anchor the Lys D6 (K109) side-chain, exposing its aliphatic core for hydrophobic packing with the aromatic rings of the pTyr mimetic and the naphthyl moieties.

The carboxamide oxygen atom of the specificity-determining $i+2$ Asn forms a hydrogen bond with the backbone amide of Lys D6 (K109) and an intramolecular hydrogen bond with its own amide to the Ac_6c residue, while its nitrogen atom is bound by the carbonyl oxygen atom of Lys D6 (K109) and Leu E4 (L120). These interactions are conserved in other Grb2 SH2 domain peptide ligands. The cyclohexyl moiety in the $i+1$ site is in van der Waals contact with Phe D5 (F108) and the aliphatic portion of Gln D3 (Q106). The carbonyl oxygen atom of His D4 (H107) is hydrogen-bonded to atom N3 of the ligand.

The protein–ligand interactions in the pTyr-binding site are identical for the $C222_1$ subunits A and C, and the *F*222 subunit A (A site), but are somewhat different for the $C222_1$ subunits B and D, and the *F*222 subunit B (B site). In the latter, the BC loop is in the open conformation, rotating the side-chains of residues Ser B7 (S88), Glu BC1 (E89), and Ser BC2 (S90) away from the ligand, resulting in a loss of four hydrogen bonds (Figure 3(b)). The water molecule W129 replaces the OG side-chain of Ser B7 (S88) in bonding to the malonyl O3. The loop movement brings Asp BC6 (D94) into the ligand-binding site to form a hydrogen bond to the NZ atom of Lys D6 (K109). Unlike its rotamer in site A, the naphthyl ring of S1s in site B flips 180° and no longer interacts with Lys D6 (K109). In this orientation, it makes van der Waals contacts with Leu D′1 (L111), Phe E3 (F119), and the naphthyl group of the S1s that binds as a dimer to the "C site" (Figure 4(a)). The side-chain of Trp EF1 (W121) flips 120° towards the α and β carbon atoms of Asn+2 from its relative position in site A and the N-terminal–CH_2CO_2H moiety of S1s rotates away from the aromatic ring of the peptide mimetic, but still maintains interactions with Arg A2 (R67). The side-chain of this residue adopts a conformation similar to that in 1FYR, making hydrogen bonds to the malonyl O atom of the pTyr mimetic with its NE atom (Figure 3(b)). The side-chain of Asn+2 is involved in the same specific interactions as in the A site. However, there is an additional intramolecular interaction between the pTyr mimetic carbonyl oxygen and atom N on the opposite side of the S1s central ring. This hydrogen bonding is also

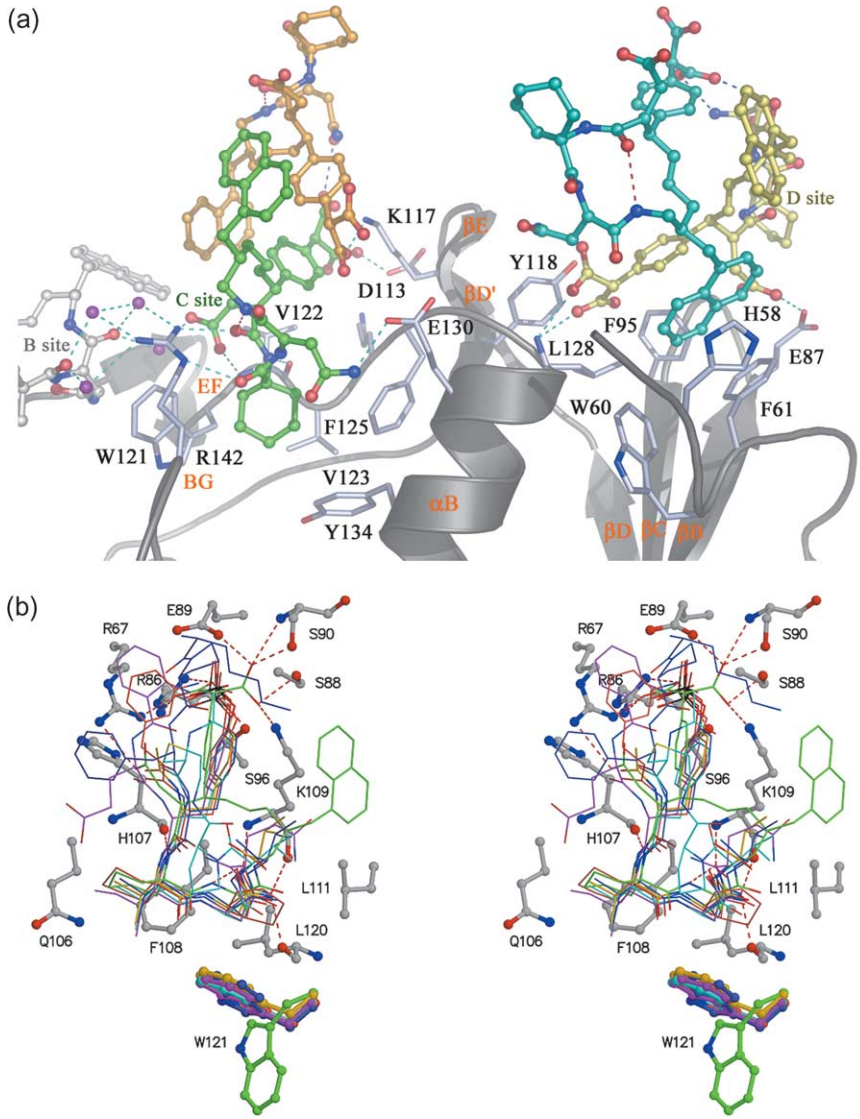

Figure 4 (a) and (b) (*legend next page*)

present in the Grb2 SH2 domain complex structures 1FYR, 1JYR, 1QG1, and 1TZE.

Brief description of the C and D sites

The Grb2 SH2 domain has not been reported to bind ligands at locations other than the conventional site in the monomeric, dimeric, or domain-swapped dimeric forms. Therefore, note was taken that one S1s molecule was shown bound to the extended swapped portion that bridges the two subunits in the *F*222 crystal structure (C site). However, in the $C222_1$ crystal, an S1s dimer binds in this site, while another one binds to an adjacent site on the same face of the molecule (D site) (Figure 4(a)). The S1s dimer interfaces are slightly different. In the former, the protomers are related by a pseudo-2-fold axis running between the pTyr mimetic portion and the naphthyl moiety. The naphthyl moieties stack on top of the respective malonyl methylene and the aromatic ring of the pTyr mimetic (Figure 4(a)). In the latter, the monomers are shifted by 3.5–4.0 Å from a pseudo-2-fold axis. This packs the naphthyl group of one molecule against the pTyr mimetic phenyl ring and the propylene chain linking the pY and pY+3, forcing the other naphthyl ring to flip 180° to avoid steric clash.

In site C, the side-chain of Trp EF1 (W121) swings toward the Asn+2 of the S1s in site B, creating space for the Ac_6c cyclohexyl group, which fits nicely into a rather tight hydrophobic pocket lined by Trp EF1 (W121), Val F1 (V123), Phe F3 (125), Tyr B8 (Y134) and the aliphatic part of Arg BG4 (R142) from the BG loop of subunit A (Figure 4(a), green). The side-chain of Arg BG4 (R142) makes two hydrogen bonds with the backbone carbonyl groups of the C-site S1s and three hydrogen bonds with three water molecules that interact with the carbonyl oxygen atoms of the B-site S1s. The fourth water molecule directly mediates the interaction between the C-site N-terminal carboxymethyl

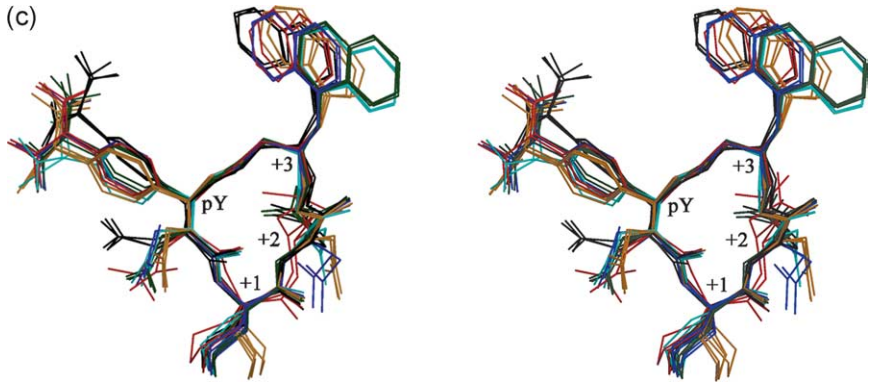

Figure 4. (a) Binding interactions between two S1s molecules and the Grb2 SH2 domain in the C site, green and orange, and D site, cyan and yellow ball-and-stick models. (b) Stereo view of the superposition of Grb2 SH2 ligands from PDB entries 1ZFP (magenta), 1FYR (gold), 1BM2 (cyan), 1TZE (slate blue), and 1CJ1 (tomato) on subunit A S1s (green). The carbon atoms of the S1s-binding residues in ball-and-stick are grey and the ligands are in bonds. Hydrogen bonds are shown in red broken lines for S1s. Superposition of all 12 S1s molecules in stereo showing different side-chain rotamers and conformational changes derived from binding in the various pockets of the domain-swapped dimer. (c) Those that bound in the A site are in black, B site in dark green, C site in orange and red, and D site in blue and cyan.

side-chain and the Asn+2 carbonyl of the B-site S1s. These four water molecules are conserved in the *F*222 structure.

Comparison of S1s with other phosphopeptidic and peptidomimetic ligands

An alignment of the α carbon traces of several Grb2 SH2 domain structures, using their core domains, shows many interesting similarities and differences between their corresponding bound ligands (Figure 4(b)). A significant shift of the Pmf side-chain as compared to that of the pTyr is necessary to position atoms O and O1 of the carboxylate group close to atoms OP2 and OP1 of the phosphate, thus preserving the bifurcated salt-bridge to Arg B5 (R86). This shift may also be attributed to differences between the phenyl rings of pTyr and Pmf residues due to differences in hybridization of the phosphoryl ester oxygen and the malonyl methylene.[27] Studies of the binding of multiple phosphate mimetics in the Src SH2 domain showed that these different groups are accommodated by the flexible phosphate recognition loop to complete the hydrogen and ionic bonding requirements for high affinity.[28] Different side-chain conformations and new binding modes are tolerated.

The aliphatic linker and the naphthyl moiety pack against the aliphatic portion of Lys D6 (K109) in the S1s complex. These hydrophobic van der Waals interactions are not observed in other structures. As expected, the specificity-determining pTyr+2 Asn residues in all complexes are quite superimposable. Val and Ile side-chains of the minimal Grb2 SH2 domain-binding tetrapeptide at the pY+1 position align well with the Ac_6c cyclohexyl moiety in both S1s and in the phosphopeptide-based complex structure 1CJ1.[29] Interestingly, atoms CA, CB, CG1, and CD1 of pTyr+1 Ile in the 1ZFP complex[12] assume a conformation that resembles half the chair of the Ac_6c cyclohexyl group. Despite the differing positions of various N-terminal capping groups such as acetyl, carboxymethyl, 3-aminobenzyloxycarbonyl (3-amino-Z), and 2-amino-benzoyl (2-Abz), their carbonyl oxygen atoms maintain hydrogen bonding or ionic interactions with the guanidino side-chain of Arg A2 (R67). The N-terminal anthranyl-based mimetics 2-Abz and 3-amino-Z, and the pTyr-1 Phe residue in the complexed structures 1ZFP, 1CJ1, 1TZE, respectively,[11,12,29] form cation/π stacking interactions with Arg A2 (R67). The stick model of the cyclic peptide cyclo-[*N*-Ac-thialysyl-pYVNVP] is shown in cyan in Figure 4(b).[30] This macrocyclic ligand follows a trajectory different from that of S1s. After Val+3, the proline residue turns away from the plane of the central ring, which is too large to be accommodated in a fashion similar to S1s.

Discussion

Conformational flexibility of S1s

It has been shown that macro-cyclization through ring closure at the phosphotyrosyl mimetic β-position enhances Grb2 SH2 binding affinity and potency in whole-cell assays.[16,21] This type of ring closure has advantages over traditional head-to-tail cyclization by reducing the degrees of rotational freedom at both ring junctures. However, a certain degree of flexibility remains in both the macrocycle skeleton and the side-chains (Figure 4(c)). Despite the seeming rigidity of the macrocycle, the aliphatic linkage between the Pmf and naphthylpropyl groups and the peptide backbone are relatively flexible. It is apparent from the alignment of 15 molecules of S1s that binding of the ligand proceeds *via* an induced-fit mechanism, such that its side-chain conformations reflect the environment of the binding pocket. Lange *et al*. showed that

similar phosphoryl-mimicking fragments such as oxalate and malonate can induce a shift in protein residues by as much as 3 Å in order to maintain a complete H-bond network in the pTyr-binding pocket.[31]

The observed ligand conformations can be grouped together according to the type of Grb2 SH2 domain binding across crystal forms. There are four major clusters of conformations based on the rotational and translational position of the Pmf residue. These are the A site S1s, consisting of $C222_1$ subunits A and C, and *F*222 subunit A; the B site S1s, consisting of $C222_1$ subunits B and D, and *F*222 subunit B; the C site S1s, consisting of ligands that bind in the swapped region between the two monomers; and the D site S1s, consisting of ligands that bind in the site opposite to the A site in the same monomer. As described earlier, the open BC loop conformation in the B site leads to a rotation of the Pmf such that the malonyl head group is displaced approximately 1 Å from its position in the A site. The Pmf rings in the C and D sites are slightly rotated but align well with those in site B, since their malonyl head groups are not as extensively bound as in the A site. The naphthyl and carboxymethyl moieties have two predominant rotamers, as exemplified by S1s in sites A and B. The Ac_6c cyclohexyl side-chain adopts two inversely related chair conformations, as exemplified by those S1s molecules that are closest to the surface of the protein in the C site (yellow in Figure 4(c)), on the one hand, and the remainder of the ligands on the other. The strong preference of the pTyr+2 Asn amide side-chain to interact with the backbone atoms of Lys D6 (K109) and Leu E4 (L120) is clearly seen for all ligands that bind in the canonical pTyr-binding site, while a variety of conformations are assumed in the other sites.

Structural differences between sites A and B

Superposition of $C222_1$ subunit B (Figure 3(b)) onto A (Figure 3(a)) not only showed differences in the conformation of the BC loop, but also in the first turn of helix αA and loop BG. In subunit B, Arg2A (R67) moves roughly 1.8 Å into the active site in response to a shift in the ligand position by ∼1.4 Å, forcing the carboxymethyl side-chain to rotate away from the Pmf. This brings the pTyr+2 Asn β-methylene to within 3.6 Å of Trp EF1 (W121), which otherwise would be 4.6 Å away. The movement also pulls the naphthyl moiety away from Lys D6 (K109), preventing it from optimal positioning. Instead, it assumes an alternative rotamer and becomes positioned into a hydrophobic groove formed by Leu βD′1 (L111) and Phe E3 (F119). Strand βD is shifted by less than 1 Å to maintain essential contacts with pTyr+2 Asn and pY+1 cyclohexyl groups.

Propensity of S1s to aggregate

Unlike other phosphopeptide, peptidomimetic, and non-peptidic ligands, the unique macrocyclic nature of S1s causes it to dimerize, perhaps upon binding to the protein. The interactions are specific and mainly hydrophobic as seen in the pseudo-2-fold binding by the two molecules in site C, and a slightly different interface in site D. Other types of interactions were observed in the contacts between S1s and symmetry-related neighbors. The C-site S1s that is away from the protein makes a 2-fold crystallographic contact with itself at the pTyr+2 Asn β carbon position. Its aliphatic ring-closing linker and the edge of its naphthyl group stack onto the naphthyl rings from the symmetry-related S1s in the active site of subunit D. The latter also interacts with the same regions of the other C-site S1s. One of the ligands in the D site (yellow in Figure 4(a)) has its naphthyl group tucked against a flat hydrophobic surface formed by Phe E3 (F62), Lys AA2 (K64), Ile AA3 (I65), Lys A4 (K69), Pro A1 (P66), and Met A8 (M73) coming from the symmetry-related subunit C.

The macrocyclic ligands bound in the canonical active site also interact with symmetry-related neighbors in both crystal forms. The B-site S1s makes contact with the aliphatic linker and naphthyl group of both symmetry-related C-site molecules with its own naphthyl group. The naphthyl group of the symmetry C-site S1s (green in Figure 4(a)) packs extensively against Lys D6 (K109) in the B-active site. S1s in the canonical A-site also forms a 2-fold interaction with the symmetry-related S1s from subunit C at the back bone near the α-carbon of the pY+1 position. Its naphthyl moiety stacks extensively parallel with symmetry-related Arg BG4 (R142) of subunit D with five points of contact between 3.4 Å and 3.5 Å apart. The same interactions were seen with the symmetry A-site S1s in subunit C and the arginine from subunit B.

Consequently, the ligands bound in the four sites in both space groups are involved in the formation of lattice contacts necessary for crystallization. This is reflected in the ease with which the Grb2 SH2/S1s complex crystallized and diffracted to a relatively high resolution. Along with S1s, other similar inhibitors were also used in an attempt to elucidate their structures. These include structure 3 (Figure 1), in which the Pmf has been replaced with a 4-(phosphonomethyl) phenylalanine (Pmp) derived pTyr mimetic and S2s, which is the same as structure 3, only the naphthyl ring has been replaced by a 5-methylindolyl group.[32] While structure 3 did not crystallize, S2s crystallized reproducibly but scattered X-rays too poorly for structure determination. It is interesting that the S2s complex crystallized as a shower of microcrystals at 18 °C but as 0.2 mm single crystals at 37 °C. Unlike phosphonate-based phosphoryl mimetics such as in structure 3, the Pmf malonyl group makes hydrogen bonds to Glu BC1 (E89) and Lys D6 (K109), and is rotated slightly, exposing the malonyl methylene and the aromatic ring for van der Waals interactions with the partner's naphthyl group as observed in

sites C and D. Regarding replacement of the naphthyl group in structure **3** with a 5-methylindolyl group, the fact that crystallization occurred strongly suggests that the crystal lattice is different from those of the S1s structures. This is indeed the case, since the space group is hexagonal rather than orthorhombic. If differences occur only in the pY+3 side-chain, the 5-methylindolyl group would be directed toward charged and polar side-chains from a symmetry-related molecule in the site A, and the indolyl nitrogen atom would be in van der Waals distance from a hydrophobic group in site B. In addition, it would be too close for either the dicarboxylic head group or the carboxylate of the N-terminal carboxymethyl side-chain in sites C and D. These unfavorable interactions would have prevented the S2s complex from crystallizing in the same manner as the S1s complex.

Prospects for further optimization of S1s

The structures reported here provide a detailed picture of the binding mode and interactions between S1s and Grb2. The prospects for further optimization of the inhibitor are limited due to the already extensive effort to improve binding affinity at the pTyr, pTyr+1, pTyr+2, and pTyr+3 positions. However, in the pTyr-binding site of $C222_1$ subunit A, the structure reveals a shallow pocket created by the side-chains of Leu D1 (L111), Phe E3 (F119), Val EF2 (V122), subunit B Arg BG4 (R142), and α and β-carbon atoms of Trp EF1 (W121). The only S1s atom pointing into this groove is pTyr+2 O4, which makes a hydrogen bond to one of three water molecules occupying the pocket. In subunit B, this pocket is partially occupied by the pTyr+3 naphthyl group, part of the S1s dimer from the C site, and water molecules. The pTyr+2 carbonyl could be modified by adding a naphthyl moiety that can bind in this shallow groove, which is a little too large for a phenyl group. It would interact with the hydrophobic side-chains surrounding the pocket and the cationic moiety of Arg BG4 (R142). In addition, by fully occupying this pocket, non-specific binding of the inhibitor in site C would be prevented.

Conclusions

We conclude that the binding of S1s in the C and D sites is a crystallographic artifact based on the presence of multiple crystal lattice contacts, symmetry-related interactions, and the fact that this has not been observed before. However, the mode of binding and interactions of S1s with the pTyr target site in Grb2 are consistent with other ligands and molecular modeling. The structures presented here reveal the molecular basis for the high-affinity binding of "second generation" inhibitors of the Grb2 SH2 domain and establish a structural framework for further optimization.

Materials and Methods

Cloning, protein expression and purification

The vector used to express residues 55–153 of Grb2 SH2 domain was constructed by Gateway recombinational cloning (Invitrogen, Carlsbad, CA). The target ORF in the expression vector pHKP1412 was amplified by PCR with a "forward" primer containing a ribosome binding site (5′-CTT TAA GAA GGA GAT ATA CAT ATG AAA CCA CAT CCG TGG TTT TTT GGC AAA ATC CCC AG−3′) and a "reverse" primer containing the attB2.1 recombination site. The purified amplicon was used as the template for a second round of PCR with another forward primer (5′-GGGG ACA ACT TTG TAC AAA AAA GTT GTG TTT AAC TTT AAG AAG GAG ATA TAC-3′) to add the attB1.1 recombination site to the amplicon upstream of the ribosome binding site and the same reverse primer that was used in the first round of PCR. The final PCR product was gel-purified and inserted by recombinational cloning into the donor vector pDONR201 (Invitrogen). The DNA sequence was confirmed experimentally, and then the ORF was recombined into the destination vector pDEST-14 (Invitrogen) to create the T7 expression vector.

The Grb2 SH2 domain was overproduced in *Escherichia coli* BL21(DE3) CodonPlus-RIL cells (Stratagene, La Jolla, CA). Single antibiotic-resistant colonies were used to inoculate 100 ml of Luria broth[33] supplemented with 100 μg ml^{-1} of ampicillin, 30 μg ml^{-1} of chloramphenicol, and 0.2% (w/v) (D+)-glucose monohydrate (Fluka). These cultures were grown by shaking (225 rev min^{-1}) to saturation overnight at 37 °C and then diluted 50-fold into several liters of fresh medium. When the cells reached early log phase ($A_{600\ nm}$=0.3–0.5), the temperature was reduced to 30°C and isopropyl β-D-thiogalactopyranoside (IPTG) was added to a final concentration of 1 mM. The cells were grown for 4 h and recovered by centrifugation at 5000*g* for 10 min and stored at −80 °C.

E. coli cell paste was suspended in ice-cold buffer A (20 mM Hepes (pH 7.2)) containing Complete EDTA-free Protease-inhibitor Cocktail (Roche Molecular Biochemicals, Indianapolis, IN). The cells were lysed with an APV Gaulin model G1000 homogenizer at 69 MPa and centrifuged at 30,000*g* for 30 min at 4 °C. The supernatant was filtered through a 0.45 μm pore size polyethersulfone membrane and applied onto a 50 ml Sulphopropyl Sepharose Fast Flow ion-exchange column (Amersham Pharmacia Biotech, Piscataway, NJ) equilibrated in buffer A. The column was washed with five column volumes of buffer A after which the bound protein was eluted with a linear gradient from 0 to 400 mM NaCl in buffer A. Fractions containing recombinant Grb2 SH2 domain as determined by SDS-PAGE were pooled and concentrated with an Amicon YM3 membrane (Millipore, Billerica, MA). The concentrate was loaded onto a 20 ml phosphotyrosyl agarose 4 CL column pre-equilibrated with ten column volumes of buffer B (20 mM Hepes (pH 7.2), 100 mM NaCl). The protein was eluted with a gradient from 0 to 150 mM Na_2HPO_4, pooled and spun down. The sample was applied to a 26/60 HiLoad Superdex 75 prep-grade column (Amersham Biosciences) equilibrated with buffer B. The sample fractionated into two peaks on this column that corresponded, according to dynamic light-scattering analysis (not shown), to monomeric and dimeric forms of the Grb2 SH2 domain. The monomer fractions were pooled and concentrated to 8–10 mg/ml. The final product was judged to be >95% pure by

SDS-PAGE (data not shown). The molecular mass was confirmed by electrospray mass spectrometry.

Crystallization of the Grb2 SH2/S1s complex and data collection

The sodium salt of S1s was dissolved in water and added to the highly pure Grb2 SH2 domain at 1.5:1 ligand to protein molar ratio. The complex was heated at 50 °C for 10 min as described by Nioche *et al.*[15] before crystallization experiments were set up. The non-heated sample also crystallized but not as well as the heated one. The crystals were grown by vapor-phase diffusion using crystallization tools from Nextal Biotechnologies. Initial screens include conditions from all the published crystal structures of Grb2 SH2 domain and its complexes. The first hit came from conditions similar to those of the Grb2 SH2/Ac-pYVNV complex.[14] These were further optimized, yielding single crystals of 0.1–0.2 mm in the longest dimension in the orthorhombic space groups *F*222 (12% polyethylene glycol (PEG)3350, 0.7 M NaCl, 100 mM $NaCH_3CO_2$ (pH 5.7)) and $C222_1$ (12% PEG3350, 1.4 M NaCl, 100 mM $NaCH_3CO_2$ (pH 5.7))(Table 1).

For both lattice types, a single large crystal was immersed in a cryo-protectant containing the mother liquor and 20% (v/v) glycerol and flashed-cooled in liquid nitrogen. The data were collected at the SER-CAT insertion device beamline 22-ID (Advanced Photon Source, Argonne National Laboratory) and reduced with the HKL 2000 suite of programs.[34] There are two Grb2 SH2 molecules in the asymmetric unit of the face-centered space group with a specific volume (V_m) of 2.7 $Å^3$/Da and solvent content of 54% (v/v), and four molecules per asymmetric unit for the C-centered one with 2.5 $Å^3$/Da and 50% (v/v), Mathews coefficient and solvent content, respectively.[35]

Structure determination and refinement

Initially, all the deposited structures of the Grb2 SH2 domain were used as search models (either as a monomer, dimer, or domain-swapped dimer) for molecular replacement (MR) with various programs, but no solutions were found. One of the models (PDB code 1ZFP) was then subjected to perturbation by normal mode analysis (NMA), an algorithm that predicts movements of a protein structure that are likely to be induced by ligand binding.[36] The templates generated by this method were input into an automatic MR program as starting models.[37] Although no definitive solutions were found, the top models from MR were refined and density maps were calculated and examined. This iterative process led to the truncation of the original model from both the N and C termini to give the fragment corresponding to residues 59–136 of Grb2. The perturbed and truncated model was subjected to automatic MR again and a borderline solution was found with an *R*-factor of 49.1%. The structure is a domain-swapped dimer with electron density observed for residues 58–150 in subunit A and 68–87, 93–149 in subunit B. The r.m.s. distance for the superposition of subunit A on B is 0.64 Å.

The refined domain-swapped dimer of *F*222 packing was placed in the unit cell of the $C222_1$ crystal for molecular replacement with the program Phaser.[38] The likelihood-enhanced fast rotation function located four strong 2-fold related peaks with a *Z* score of 20 (a score of 8 is considered a good solution). After both dimers were placed, the score increased to 59 and 58 for the two solutions, respectively. Strong density was observed for residues 56–151 of subunits A and C, and residues 59–151 of subunits B and D. The side-chains of the N-terminal residues 64–78, the first few turns of helix αA, and the BG loop of subunit D and to a lesser extent, subunit B are disordered in the structure.

Table 1. Data collection, molecular replacement, and refinement statistics

	$C222_1$	*F*222
A. *Data collection*		
X-ray source	ID-22 (APS)	ID-22 (APS)
Wavelength (Å)	0.9795	0.9795
Cell dimensions (Å)	$a=87.8$, $b=106.2$, $c=102.1$	$a=88.2$, $b=102.7$, $c=107.2$
Resolution (Å)	25–1.78	20–2.0
Unique reflections	45,886	15,744
Completeness (%)	99.7	94.0
Redundancy	7.3	5.0
I/σ (last shell)	27 (2.1)	18 (1.8)
R_{sym}[a] (last shell)	0.065 (0.55)	0.067 (0.52)
Mean *B* value ($Å^2$)	35.0	40
B. *Molecular replacement*		
R-factor (%)	49.1	
Z score		59.0
Number of reflections	42,084	14,945
C. *Refinement*		
R_{cryst}[b] (%)	23.2	24.5
R_{free}[c] (%)	29.3	30.7
r.m.s. deviation from ideal geometry		
Bond lengths (Å)	0.022	0.044
Bond angles (deg.)	3.03	3.7
Number of molecules		
Polypeptide	4	2
Ligand	12	3
Polyethylene glycol		1
Water	375	103

[a] $R_{sym}=(\Sigma_h(I_h-\langle I\rangle()/(\Sigma_h I_h)$.
[b] $R_{cryst}=(\Sigma_h(F_{obs}-F_{cal}()/(\Sigma_h F_{obs})$.
[c] R_{free}=crystallographic *R*-factor for test set as implemented in Refmac_5.2.[40]

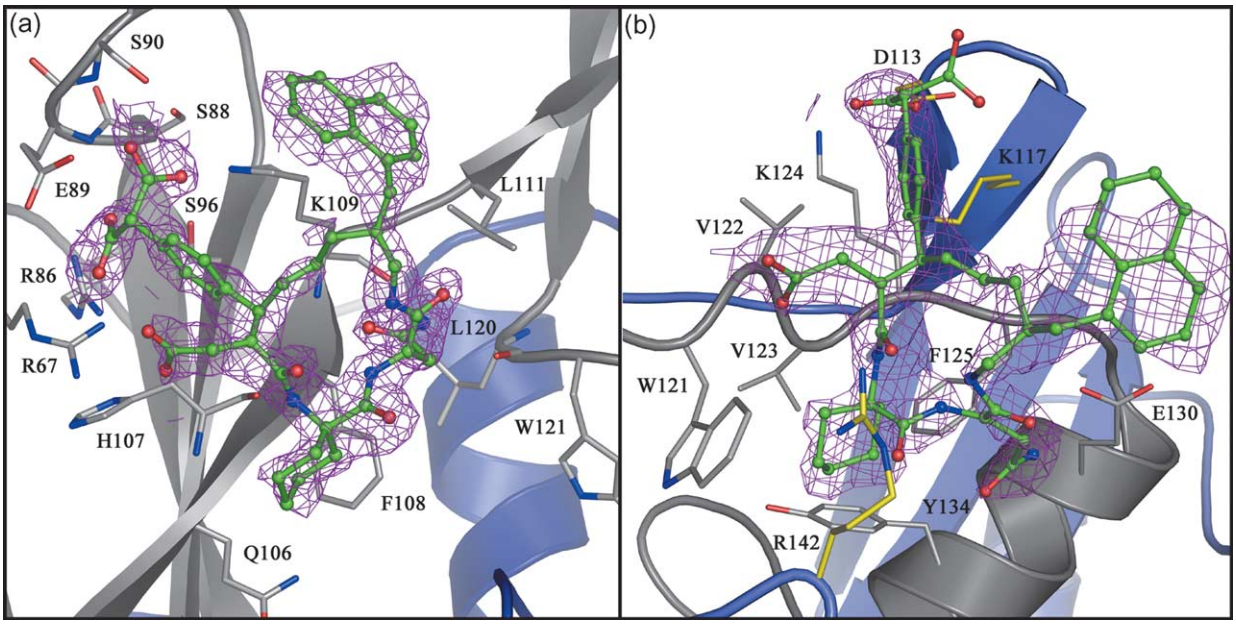

Figure 5. (a) The omit density map superimposed on the final model of the inhibitor in the active site of subunit C, space group $C222_1$ and (b) site C of space group $F222$, contoured at 1.2σ. The protein residues are depicted in bonds and ligands in ball-and-stick. The ligand binding side-chains in site C from subunit B have grey carbon atoms and those from subunit A are yellow.

The ligand density was located in the traditional binding sites of the SH2 domains as well as in additional sites in the swapped region between the two molecules and in subunits A and C of the $C222_1$ crystal. A model of the inhibitor was built, energy minimized, and positioned into the density (Sybyl 6.9; Tripos). The omit maps of the ligand in the active site and an additional site are shown in Figure 5. Visual inspection and manual building of the model was accomplished with the graphics program O.[39] The structures were refined using Refmac5 with TLS parameters assigned to the core and swapped domains for the refinement of anisotropic displacements.[40] All Figures were prepared using the graphics program PyMOL,[41] except for Figure 4(b) and (c), which were made with MOLSCRIPT[42] and rendered with Raster3D.[43]

Protein Data Bank accession codes

The atomic coordinates and structure factors for the $C222_1$ and $F222$ structures were deposited in the RCSB Protein Data Bank[44] with accession codes 2AOB and 2AOA, respectively.

Acknowledgements

This research was supported by the Intramural Research Program of the NIH, National Cancer Institute, Center for Cancer Research. We thank Howard Peters, Scott Cherry, and Joseph Tropea for early contributions to this work and the SBL Biophysics Core Resource (US National Cancer Institute at Frederick) for the use of the electrospray mass spectrometer. X-ray diffraction data were collected at the Southeast Regional Collaborative Access Team (SER-CAT) 22-ID beamline at the Advanced Photon Source, Argonne National Laboratory (supporting institutions may be found at www.ser-cat.org/members.html). Use of the Advanced Photon Source was supported by the US Department of Energy, Office of Science, Office of Basic Energy Sciences, under contract no. W-31-109-Eng-38.

References

1. Shawver, L. K., Slamon, D. & Ullrich, A. (2002). Smart drugs: tyrosine kinase inhibitors in cancer therapy. *Cancer Cell*, **1**, 117–123.
2. Marshall, J. L., Kindler, H., Deeken, J., Bhargava, P., Vogelzang, N. J., Rizvi, N. *et al*. (2005). Phase I trial of orally administered CEP-701, a novel neurotrophin receptor-linked tyrosine kinase inhibitor. *Invest. New Drugs*, **23**, 31–37.
3. Pawson, T., Raina, M. & Nash, P. (2002). Interaction domains: from simple binding events to complex cellular behavior. *FEBS Letters*, **513**, 2–10.
4. Dankort, D., Maslikowski, B., Warner, N., Kanno, N., Kim, H., Wang, Z. *et al*. (2001). Grb2 and Shc adapter proteins play distinct roles in Neu (ErbB-2)-induced mammary tumorigenesis: implications for human breast cancer. *Mol. Cell Biol.* **21**, 1540–1551.
5. Furge, K. A., Zhang, Y. W. & Vande Woude, G. F. (2000). Met receptor tyrosine kinase: enhanced signaling through adapter proteins. *Oncogene*, **19**, 5582–5589.
6. Sawyer, T. K., Bohacek, R. S., Dalgarno, D. C., Eyermann, C. J., Kawahata, N., Metcalf, C. A., 3rd *et al*. (2002). SRC homology-2 inhibitors: peptidomimetic and nonpeptide. *Mini Rev. Med. Chem.* **2**, 475–488.

7. Vu, C. B. (2000). Recent advances in the design and synthesis of SH2 inhibitors of Src Grb2 and ZAP-70. *Curr. Med. Chem.* **7**, 1081–1100.
8. Fretz, H., Furet, P., Garcia-Echeverria, C., Schoepfer, J. & Rahuel, J. (2000). Structure-based design of compounds inhibiting Grb2-SH2 mediated protein-protein interactions in signal transduction pathways. *Curr. Pharm. Des.* **6**, 1777–1796.
9. Ogura, K., Tsuchiya, S., Terasawa, H., Yuzawa, S., Hatanaka, H., Mandiyan, V. *et al*. (1999). Solution structure of the SH2 domain of Grb2 complexed with the Shc-derived phosphotyrosine-containing peptide. *J. Mol. Biol.* **289**, 439–445.
10. Yuzawa, S., Yokochi, M., Hatanaka, H., Ogura, K., Kataoka, M., Miura, K. *et al*. (2001). Solution structure of Grb2 reveals extensive flexibility necessary for target recognition. *J. Mol. Biol.* **306**, 527–537.
11. Rahuel, J., Gay, B., Erdmann, D., Strauss, A., Garcia-Echeverria, C., Furet, P. *et al*. (1996). Structural basis for specificity of Grb2-SH2 revealed by a novel ligand binding mode. *Nature Struct. Biol.* **3**, 586–589.
12. Rahuel, J., Garcia-Echeverria, C., Furet, P., Strauss, A., Caravatti, G., Fretz, H. *et al*. (1998). Structural basis for the high affinity of amino-aromatic SH2 phosphopeptide ligands. *J. Mol. Biol.* **279**, 1013–1022.
13. Tsuchiya, S., Ogura, K., Hatanaka, H., Nagata, K., Terasawa, H., Mandivan, V. *et al*. (1999). Solution structure of the SH2 domain of Grb2/Ash complexed with EGF receptor-derived phosphotyrosine containing peptide. *J. Biochem. (Tokyo)*, **125**, 1151–1159.
14. Schiering, N., Casale, E., Caccia, P., Giordano, P. & Battistini, C. (2000). Dimer formation through domain swapping in the crystal structure of the Grb2-SH2-Ac-pYVNV complex. *Biochemistry*, **39**, 13376–13382.
15. Nioche, P., Liu, W. Q., Broutin, I., Charbonnier, F., Latreille, M. T., Vidal, M. *et al*. (2002). Crystal structures of the SH2 domain of Grb2: highlight on the binding of a new high-affinity inhibitor. *J. Mol. Biol.* **315**, 1167–1177.
16. Shi, Z. D., Wei, C. Q., Lee, K., Liu, H., Zhang, M., Araki, T. *et al*. (2004). Macrocyclization in the design of non-phosphorus-containing Grb2 SH2 domain-binding ligands. *J. Med. Chem.* **47**, 2166–2169.
17. Waksman, G., Shoelson, S. E., Pant, N., Cowburn, D. & Kuriyan, J. (1993). Binding of a high affinity phosphotyrosyl peptide to the Src SH2 domain: crystal structures of the complexed and peptide-free forms. *Cell*, **72**, 779–790.
18. Eck, M. J., Shoelson, S. E. & Harrison, S. C. (1993). Recognition of a high-affinity phosphotyrosyl peptide by the Src homology-2 domain of p56lck. *Nature*, **362**, 87–91.
19. Lee, C. H., Kominos, D., Jacques, S., Margolis, B., Schlessinger, J., Shoelson, S. E. & Kuriyan, J. (1994). Crystal structures of peptide complexes of the amino-terminal SH2 domain of the Syp tyrosine phosphatase. *Structure*, **2**, 423–438.
20. Garcia-Echeverria, C., Furet, P., Gay, B., Fretz, H., Rahuel, J., Schoepfer, J. & Caravatti, G. (1998). Potent antagonists of the SH2 domain of Grb2: optimization of the X+1 position of 3-amino-Z-Tyr(PO3H2)-X+1-Asn-NH2. *J. Med. Chem.* **41**, 1741–1744.
21. Furet, P., Gay, B., Caravatti, G., Garcia-Echeverria, C., Rahuel, J., Schoepfer, J. & Fretz, H. (1998). Structure-based design and synthesis of high affinity tripeptide ligands of the Grb2-SH2 domain. *J. Med. Chem.* **41**, 3442–3449.
22. Wei, C. Q., Gao, Y., Lee, K., Guo, R., Li, B., Zhang, M. *et al*. (2003). Macrocyclization in the design of Grb2 SH2 domain-binding ligands exhibiting high potency in whole-cell systems. *J. Med. Chem.* **46**, 244–254.
23. Gao, Y., Luo, J., Yao, Z. J., Guo, R., Zou, H., Kelley, J. *et al*. (2000). Inhibition of Grb2 SH2 domain binding by non-phosphate-containing ligands 2. 4-(2-malonyl)-phenylalanine as a potent phosphotyrosyl mimetic. *J. Med. Chem.* **43**, 911–920.
24. Shakespeare, W., Yang, M., Bohacek, R., Cerasoli, F., Stebbins, K., Sundaramoorthi, R. *et al*. (2000). Structure-based design of an osteoclast-selective, nonpeptide src homology 2 inhibitor with *in vivo* antiresorptive activity. *Proc. Natl Acad. Sci. USA*, **97**, 9373–9378.
25. Sundaramoorthi, R., Kawahata, N., Yang, M. G., Shakespeare, W. C., Metcalf, C. A., 3rd & Wang, Y. (2003). Structure-based design of novel nonpeptide inhibitors of the Src SH2 domain:phosphotyrosine mimetics exploiting multifunctional group replacement chemistry. *Biopolymers*, **71**, 717–729.
26. Bohacek, R. S., Dalgarno, D. C., Hatada, M., Jacobsen, V. A., Lynch, B. A., Macek, K. J. *et al*. (2001). X-ray structure of citrate bound to Src SH2 leads to a high-affinity, bone-targeted Src SH2 inhibitor. *J. Med. Chem.* **44**, 660–663.
27. Tong, L., Warren, T. C., Lukas, S., Schembri-King, J., Betageri, R., Proudfoot, J. R. & Jakes, S. (1998). Carboxymethyl-phenylalanine as a replacement for phosphotyrosine in SH2 domain binding. *J. Biol. Chem.* **273**, 20238–20242.
28. Lange, G., Lesuisse, D., Deprez, P., Schoot, B., Loenze, P., Benard, D. *et al*. (2002). Principles governing the binding of a class of non-peptidic inhibitors to the SH2 domain of src studied by X-ray analysis. *J. Med. Chem.* **45**, 2915–2922.
29. Furet, P., Garcia-Echeverria, C., Gay, B., Schoepfer, J., Zeller, M. & Rahuel, J. (1999). Structure-based design, synthesis, and X-ray crystallography of a high-affinity antagonist of the Grb2-SH2 domain containing an asparagine mimetic. *J. Med. Chem.* **42**, 2358–2363.
30. Ettmayer, P., France, D., Gounarides, J., Jarosinski, M., Martin, M. S., Rondeau, J. M. *et al*. (1999). Structural and conformational requirements for high-affinity binding to the SH2 domain of Grb2(1). *J. Med. Chem.* **42**, 971–980.
31. Lange, G., Lesuisse, D., Deprez, P., Schoot, B., Loenze, P., Benard, D. *et al*. (2003). Requirements for specific binding of low affinity inhibitor fragments to the SH2 domain of (pp60)Src are identical to those for high affinity binding of full length inhibitors. *J. Med. Chem.* **46**, 5184–5195.
32. Shi, Z. D., Lee, K., Wei, C. Q., Roberts, L. R., Worthy, K. M., Fisher, R. J. & Burke, T. R., Jr (2004). Synthesis of a 5-methylindolyl-containing macrocycle that displays ultrapotent Grb2 SH2 domain-binding affinity. *J. Med. Chem.* **47**, 788–791.
33. Miller, J. H. (1972). *Experiments in Molecular Genetics*, Cold Spring Harbor Laboratory Press, Cold Spring Harbor, NY.
34. Otwinowski, Z. & Minor, W. (1997). Processing of X-ray Diffraction Data Collected in Oscillation Mode. *Methods Enzymol.* **276A**, 307–326.
35. Matthews, B. W. (1968). Solvent content of protein crystals. *J. Mol. Biol.* **33**, 491–497.
36. Suhre, K. & Sanejouand, Y. H. (2004). On the potential of normal-mode analysis for solving difficult molecular-replacement problems. *Acta Crystallog. sect. D*, **60**, 796–799.

37. Collaborative Computing Project, Number 4 (1994). The CCP4 suite: programs for protein crystallography. *Acta Crystallog. sect. D*, **50**, 760-763.
38. Storoni, L. C., McCoy, A. J. & Read, R. J. (2004). Likelihood-enhanced fast rotation functions. *Acta Crystallog. sect. D*, **60**, 432–438.
39. Jones, T. A., Zou, J. Y., Cowan, S. W. & Kjeldgaard, S. S (1991). Improved methods for building protein models in electron density maps and the location of errors in these models. *Acta Crystallog. sect. A*, **47**, 110–119.
40. Murshudov, G. N., Vagin, A. A. & Dodson, E. J. (1997). Refinement of macromolecular structures by the maximum-likelihood method. *Acta Crystallog. sect. D*, **53**, 240–255.
41. DeLano, W. L. (2002). *The PyMOL Molecular Graphics System*, Delano Scientific, San Carlos, CA.
42. Kraulis, P. J. & title (1991). MOLSCRIPT: a program to produce both detailed and schematic plots of protein structures. *J. Appl. Crystallog.* **24**, 946–950.
43. Merritt, E. A. & Murphy, M. E. P. (1994). Raster3D version 2.0. A program for photorealistic molecular graphics. *Acta Crystallog. sect. D*, **50**, 869–873.
44. Berman, H. M., Westbrook, J., Feng, Z., Gilliland, G., Bhat, T. N., Weissig, J. *et al*. (2000). The Protein Data Bank. *Nucl. Acids Res.* **28**, 235–242.

Edited by I. Wilson

(Received 24 May 2005; received in revised form 15 August 2005; accepted 17 August 2005)
Available online 2 September 2005